Available online at www.sciencedirect.com

Thermochimica Acta 415 (2004) 47–54

thermochimica acta

www.elsevier.com/locate/tca

Thermophysical properties of solid and liquid platinum

B. Wilthan, C. Cagran, C. Brunner, G. Pottlacher*

Institut für Experimentalphysik, Technische Universität Graz, Petersgasse 16, 8010 Graz, Austria

Received 5 May 2003; accepted 26 June 2003

Abstract

With ohmic pulse heating the measurement of thermophysical data of electrically conducting materials far into the fluid stage are possible. Heating rates up to 10^8 K/s are achieved, and the fluid state is achieved after about 30 μs. Within this short time the geometry of the sample will neither be destroyed through force of gravity, instabilities nor other effects, so that short-term measurements become possible at "standing" fluid columns. The values of heat capacity and enthalpy of platinum in the solid state, obtained by ohmic pulse heating, are complemented with measurements of a differential scanning calorimeter in the temperature range 473–1573 K.

Measured data are the current through the sample, the voltage drop across the sample, the radiation temperature and normal spectral emissivity at 684.5 nm. These data are evaluated and one obtains enthalpy, specific heat capacity, electrical resistivity and thermal conductivity as a function of temperature up to 3000 K.

Keywords: Thermophysical; Enthalpy; Platinum

---

1. Introduction

Platinum is a precious metal and appertains to the group of platinum metals. Its electron configuration is $[Xe]4f^{14}5d^9 6s^1$, its ordinal 78 and its relative atomic weight conducts after [1,2] 195.08. Its crystal structure is face-cubic-centered (f.c.c.). It is shiny, forge and workable and occurs in the crust of the earth with a frequency of approx. 0.001 ppm. Platinum is attacked neither of oxygen nor of water and is insoluble in all acids, with the exception of aqua regia or melted alkalis. After [2] it has the ability to include in fixed solution lot of gases, especially hydrogen and oxygen.

Platinum is used in many fields, such as for weights and standard measures, in electronic industry for electric contacts which can be exposed to high temperatures, and for the production of electrodes that can be exposed to chemicals. Particularly important is the use of platinum in exhaust catalysts, where the ceramic honeycomb structures are coated with platinum. Platinum is also employed as material in large areas of the thermodynamic temperature scale ITS-90 in platinum resistance thermometers. Further details of platinum and its alloys are found in [2].

Fast pulse-heating techniques allow the measurement of thermophysical properties of solid and liquid metals and alloys at temperatures inaccessible to most other techniques. Pulse heating involves high heating rates up to 10^8 K/s which leads to short measurement times (μs). This minimizes chemical interactions between the sample and its environment during the experiment. Over the last years we have performed pulse-heating experiments on numerous elements and alloys [3,4].

A major improvement was successfully added to our experimental set-up by the direct measurement of material optical properties, including emissivity, in the liquid phase. The emissivity measurements are performed by combining a fast laser polarimetry technique (μs-Division of Amplitude Photopolarimeter [μ-DOAP]) with our established set-up for high speed measurements on liquid metal samples at high temperatures [5].

2. Experimental

The wire-shaped platinum samples (99.99+% [6]) had a typical diameter of 0.5 mm and a typical length of 50 mm for the pulse heating, the samples for the DSC had 5.2 mm diameter and 0.5 mm of height. The density at room temperature is according to [6] 21.450 kg/m^3, the melting tem-

---

* Corresponding author. Tel.: +43-316-873-8149; fax: +43-316-873-8655.

E-mail address: pottl@eip.tu-graz.ac.at (G. Pottlacher).

0040-6031/$ – see front matter © 2004 Elsevier B.V. All rights reserved.
doi:10.1016/j.tca.2003.06.003

perature is 2042 K [7–9]. The samples are resistively volume heated in a nitrogen atmosphere at 1 bar pressure up to the end of the liquid phase by passing a large current pulse through them. The energy used for pulse heating is stored in a capacitor bank (540 μF, 10 000 V_{max}). Time resolved quantities measured are current, $I(t)$, through the sample by means of a Pearson-current monitor, voltage drop across it by means of two knife-edge probes, $U(t)$, radiation temperature, $T_{rad}(t)$, of the sample by means of a calibrated fast pyrometer working on an effective wavelength of 650 nm with a full-width-at-half-maximum (FWHM) bandwidth of 37 nm and normal spectral emissivity at 684.5 nm by means of a polarimeter (μ-DOAP), $\varepsilon(t)$. Due to the short time-scale this polarimeter has to operate without any moving parts, which is realized by dividing the intensity of the reflected beam by suitable optical components into four beams and detecting the four intensities [8]. By using an instrument matrix (a 4 × 4 array, obtained by calibration), the Stokes vector and hence full information about the polarization state of the reflected beam is obtained. The polarimeter detects changes of the polarization state of a laser beam (684.5 nm) reflected by the sample surface during the pulse-heating experiments. The change in the polarization state is used to determine the index of refraction, n, and the extinction coefficient k. This leads to the reflectivity R, of the sample and by means of Kirchhoff's law for opaque materials to the temperature dependence of normal spectral emissivity, ε.

Combining all measurements allows the determination of enthalpy, heat capacity and electrical resistivity as a function of temperature in the melting region and in the liquid phase. Thermal conductivity and thermal diffusivity are estimated using the Wiedemann–Franz law.

The DSC measurements of specific heat capacity are performed with a NETZSCH DSC 404 in the temperature range 473–1573 K under an argon atmosphere on disc-shaped samples with a diameter of 5.2 mm and a height of 0.5 mm. The results are combined with those of the pulse heating experiments.

3. Data evaluation—pulse heating

The voltages $U(t)$ used in the calculations are the measured values corrected for inductive contributions. The specific enthalpy, $H(t)$, is calculated from $U(t)$ and $I(t)$, starting at room temperature ($T = 298$ K):

$$H(t) = \frac{1}{m}\int I(t)U(t)\,\mathrm{d}t \qquad (1)$$

where m is the mass of the sample and t the time.

The electrical resistivity, $\rho_{el,uncorr}$, without volume correction may be calculated from:

$$\rho_{el,uncorr}(t) = \frac{U(t)\pi r_0^2}{I(t)l} \qquad (2)$$

where r_0 is the sample radius at room temperature, and l the length of the specimen. Considering the sample expansion $r(t)$ during heating we obtain the volume adjusted, actual resistivity from:

$$\rho_{el,corr}(t) = \rho_{el,uncorr}\frac{r^2(t)}{r_0^2} \qquad (3)$$

The resistivity measurements also start from room temperature. When using ohmic pulse heating, thermal conductivity λ, may be estimated from temperature dependent electrical resistivity, $\rho_{el,corr}$, with the help of the Wiedemann–Franz law:

$$\lambda(T) = \frac{LT}{\rho_{el,corr}(T)} \qquad (4)$$

where T is the temperature and L the Lorentz number, $L = 2.45 \times 10^{-8}\,V^2/K^2$ [7], assuming that the Lorentz number is invariant within the region of interest. Thermal diffusivity a, may be estimated from specific heat capacity at constant pressure c_p, and temperature dependent density ρ_d, using again the Wiedemann–Franz law:

$$a(T) = \frac{\lambda(T)}{c_p(T)\rho_d(T)} \qquad (5)$$

Temperature is one of the important quantities to be determined when investigating thermophysical properties of metals by pulse-heating techniques. Most of the optical pyrometers used for temperature measurements are only sensitive to temperatures above 1000 K. The radiation temperature of the sample is obtained using the voltage output of a calibrated pyrometer:

$$T_{rad} = c_2\left[\lambda \ln\left(\frac{K}{S}+1\right)\right]^{-1} \qquad (6)$$

where S is the output signal of the pyrometer, T_{rad} the radiation temperature of the sample at the effective wavelength λ of the pyrometer, K the calibration-factor of the pyrometer system, and c_2 the second radiation constant. The true sample temperature T can be obtained with the help of Planck's law by the following equation:

$$T = \frac{c_2}{\lambda\{\ln[\varepsilon\langle\exp(c_2/\lambda T_{rad}) - 1\rangle + 1]\}} \qquad (7)$$

where ε is the normal spectral emissivity at the wavelength λ. One needs the actual value of the normal spectral emissivity at the wavelength of the pyrometer used for this procedure.

The effective wavelength of a pyrometer is temperature dependent, but its dependence is omitted in the succeeding presentation. Furthermore, no correction was applied to the data to account for small differences in operating wavelengths between the pyrometer (650 nm) and the polarimeter (684.5 nm) that delivers the emissivity.

4. Data evaluation—DSC

The DSC allows to measure the heat capacity of the sample in a certain temperature range. One experiment consists usually of three separate runs: a scan with two empty pans, a scan with one pan containing a reference sample from sapphire and a scan with the sample in the same pan where the reference was before. The temperature dependent heat capacity of the sample, $c_p(T)$, is obtained in the following way:

$$c_p(T) = c_p^{\mathrm{r}}(T)\frac{m^{\mathrm{r}}}{m}\frac{\Delta_3 - \Delta_1}{\Delta_2 - \Delta_1} \qquad (8)$$

where Δ_1, Δ_2, Δ_3 are the three DSC signals with the empty pans, the reference sample and the sample. m^{r} and m are the masses of the reference sample and the sample, respectively, c_p^{r} is the heat capacity of the reference sample and T the temperature. From the DSC-measured c_p we obtain the enthalpy H using the following equation:

$$H_{298}(T) = \int_{473}^{T} c_p(T)\,\mathrm{d}T + (473 - 298)c_p(473) \qquad (9)$$

where $H(T)$ is the enthalpy and c_p the specific heat capacity.

Inverting Eq. (9) we obtain a $T(H)$-relation, which we also obtain from pulse heating in higher temperature regions. Thus we use the DSC results to assign a temperature to the corresponding enthalpy of the pulse-heating experiment. This way it is possible to enlarge the temperature range of the graphs enthalpy versus temperature and resistivity versus temperature, as can be seen in Figs. 3 and 4.

5. Results

In Fig. 1 the time dependence of normal spectral emissivity, "true temperature" and temperature calculated with a constant emissivity at melting and in the liquid phase (see [10] for details of the two approaches) for platinum versus time is depicted for a single experiment. Beginning and end of melting are indicated with two vertical lines (dotted, dashed). Within this work the melting temperature of 2042 K is used for further calculations. 27 μs after the start of the experiment (at 200 μs) a maximum temperature of about 3000 K is reached. The pyrometric obtained temperature starts at about 1500 K, because the pyrometer used (Si-Diode at 650 nm) is not sensitive below this temperature.

In Fig. 2 normal spectral emissivity ε of platinum at a wavelength of 684.5 nm versus temperature is shown and compared to literature data. The melting temperature, T_{m}, at 2042 K is indicated by a vertical dotted line. Eight measurements deliver the following linear fit for normal spectral emissivity in the temperature range from $2040\,\mathrm{K} < T < 2900\,\mathrm{K}$ is

$$\varepsilon = 0.352 + 5.233 \times 10^{-6} T \qquad (10)$$

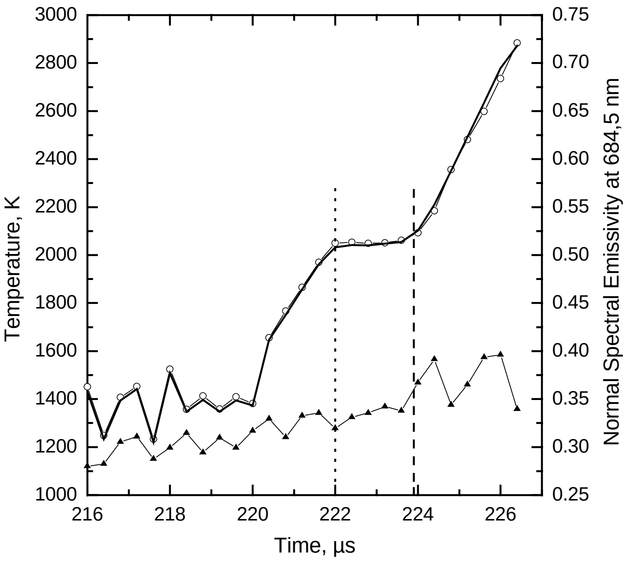

Fig. 1. Temperature and normal spectral emissivity at a wavelength of 684.5 nm for a single experiment on platinum versus time. Full triangles: normal spectral emissivity; open circles: "true temperature"; full line: temperature calculated under the assumption of a constant emissivity for the whole temperature range. Vertical dotted line: onset of melting; vertical dashed line: end of melting.

At the onset of melting a value of about $\varepsilon = 0.327$ is observed within this work, whereas at the end of melting an emissivity value of 0.363 is obtained. Righini and Rosso [11] obtain at 2000 K a value of 0.319 for a wavelength of 659 nm, McClure et al. [12] report for melting a value of

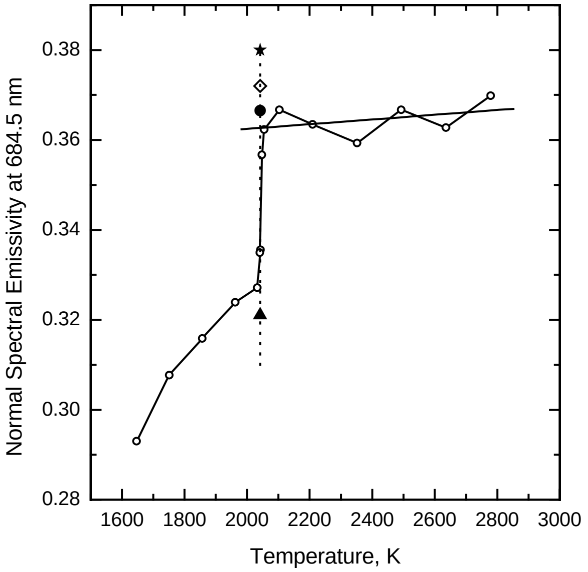

Fig. 2. Normal spectral emissivity of platinum at 684.5 nm versus temperature. Open circles: measured data from this work (average of seven measurements). Full line: linear least-squares fit to mean values for the liquid phase; open diamonds: literature value of Krishnan et al. [13]; full circle: value of McClure et al. [12]; full triangle: value of Righini and Rosso [11]; full star: value of Baykara et al. [23], vertical dotted line: melting temperature (2042 K).

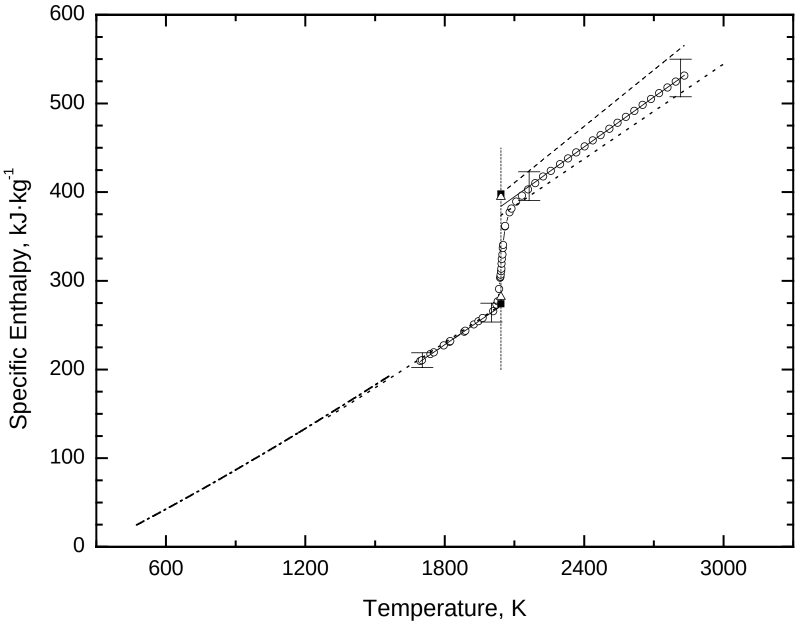

Fig. 3. Specific enthalpy versus temperature for platinum. Open circles: measured data from this work (average of 11 measurements). Full lines: linear least-squares fits to mean values of measured data; full squares: values at the begin and the end of melting from [17]; dashed line: literature values for the liquid phase from [17]; vertical dotted line: melting temperature (2042 K); open triangle: literature value from [18] at the melting temperature; dotted line: literature values from [15]; dashed-dotted line: data from this work (DSC measurement).

0.349 at 657 nm, and Krishnan et al. [13] report or the liquid at 650 nm a value of 0.38. For liquid platinum a slightly increase of normal spectral emissivity up to 2900 K is observed. All reference values in Fig. 2 have been extrapolated to a wavelength of 684.5 nm and to the melting temperature for comparison reasons.

In Fig. 3 specific enthalpy versus temperature is shown. In the temperature range from $473\,\text{K} < T < 1573\,\text{K}$ we obtain from our DSC measurements the following fit:

$$H = -38.6891 + 0.1274T + 1.3443 \times 10^{-5}T^2 \qquad (11)$$

The linear fit for solid platinum in the temperature range $1700\,\text{K} < T < 2040\,\text{K}$ is obtained from 11 independent pulse heating measurements:

$$H = -96.0750 + 0.180035T \qquad (12)$$

where H is in $\text{kJ}\,\text{kg}^{-1}$ and T in K.

For the solid we acquire a c_p value of $180\,\text{J}\,\text{kg}^{-1}\,\text{K}^{-1}$ in the range 1700–2040 K. Seville [14] reports a value of $187.5\,\text{J}\,\text{kg}^{-1}\,\text{K}^{-1}$ at 1850 K, Righini and Rosso [11] report a value of $189\,\text{J}\,\text{kg}^{-1}\,\text{K}^{-1}$ at 2000 K, and at the onset of melting Hultgren et al. [15] report $179.6\,\text{J}\,\text{kg}^{-1}\,\text{K}^{-1}$.

For the liquid in the temperature range $2045\,\text{K} < T < 2830\,\text{K}$ we obtain again from 11 pulse heating measurements

$$H = 1.63634 + 0.187235T \qquad (13)$$

where H is in $\text{kJ}\,\text{kg}^{-1}$ and T in K. For the liquid we acquire a c_p value of $187\,\text{J}\,\text{kg}^{-1}\,\text{K}^{-1}$, Margrave's review [9] reports a value of $186.7\,\text{J}\,\text{kg}^{-1}\,\text{K}^{-1}$, Chaudhuri et al. [16] report a value of $186\,\text{J}\,\text{kg}^{-1}\,\text{K}^{-1}$ obtained from levitation calorimetry, Hixson and Winkler [17] report $211.9\,\text{J}\,\text{kg}^{-1}\,\text{K}^{-1}$ at a pressure of 2000 bar obtained by pulse heating and, the data-book of Hultgren et al. [15] recommends $178.1\,\text{J}\,\text{kg}^{-1}\,\text{K}^{-1}$.

During the melting transition, which is indicated in Fig. 3 by a vertical dotted line, the specific enthalpy changes from $H_\text{s} = 271.6\,\text{kJ}\,\text{kg}^{-1}$ (index s: solid) to $H_\text{l} = 384.0\,\text{kJ}\,\text{kg}^{-1}$ (index l: liquid) yielding $\Delta H = 112.4\,\text{kJ}\,\text{kg}^{-1}$ for the latent heat of fusion. For comparison values at the melting transition from other authors are summarized in Table 1.

Fig. 4 presents electrical resistivity not corrected for thermal expansion as a function of temperature. At the onset of melting, which is indicated with a vertical dotted line, we obtain a value of $0.610\,\mu\Omega\,\text{m}$ and at the end of melting a value of $0.909\,\mu\Omega\,\text{m}$, thus an increase of $\Delta\rho = 0.299\,\mu\Omega\,\text{m}$ at melting is observed. At 2000 K, Righini and Rosso [11] report a value of $0.6171\,\mu\Omega\,\text{m}$, Martynyuk and Tsapkov [18] report for the onset of melting as $0.621\,\mu\Omega\,\text{m}$ and for the end of melting as $0.926\,\mu\Omega\,\text{m}$. In the temperature range from

Table 1
Values at the melting transition of platinum as given from different authors

Author	T (K)	H_s ($\text{kJ}\,\text{kg}^{-1}$)	H_l ($\text{kJ}\,\text{kg}^{-1}$)	ΔH ($\text{kJ}\,\text{kg}^{-1}$)
This work	2042	271.6	384.0	112.4
Chaudhuri et al. [16]	2045	–	–	113.7
Margrave [9]	2042	–	–	113.8
Hixson and Winkler [17]	2042	274	398	124
Martynyuk and Tsapkov [18]	At melting	281.9	394.7	112.8
Lebedev et al. [19]	At melting	–	–	128
Hultgren et al. [15]	2042	273.1	373.9	100.8

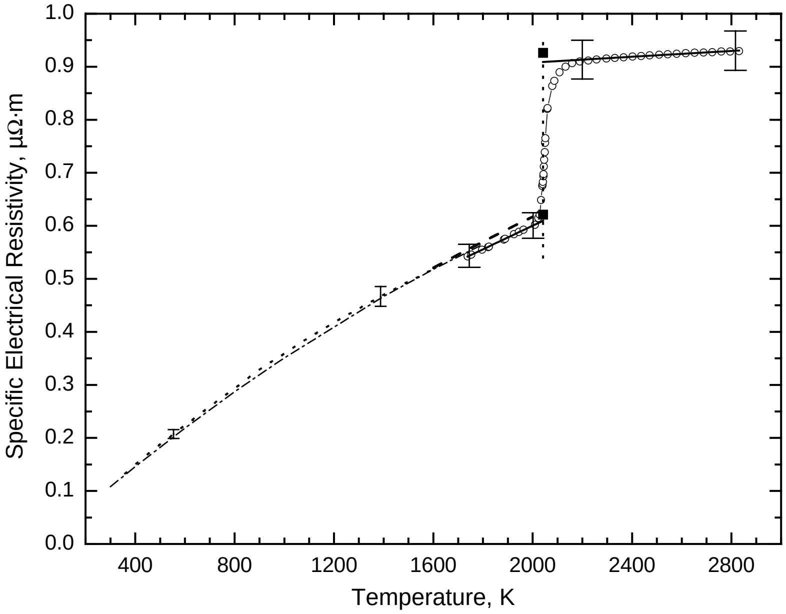

Fig. 4. Specific electrical resistivity without correction for volume expansion versus temperature for platinum. Open circles: measured pulse heating data from this work (average of 11 measurements). Full line: linear least-squares fits; vertical dotted line: melting temperature; dashed line: literature values from [11]; dashed-dotted line: literature values from [21]; full squares: values from [18]; dotted line: measured from this work with temperature from DSC measurement.

$473\,\mathrm{K} < T < 1573\,\mathrm{K}$ we obtain from our DSC measurements the following fit:

$$\rho = -0.0182 + 4.4636 \times 10^{-4}T - 6.955 \times 10^{-8}T^2 \quad (14)$$

The linear fit to our values for the solid in the temperature range $1740\,\mathrm{K} < T < 2042\,\mathrm{K}$ is

$$\rho = 0.1545 + 2.2287 \times 10^{-4}T \quad (15)$$

and for the liquid in the temperature range $2042 < T < 2900\,\mathrm{K}$

$$\rho = 0.8537 + 2.7129 \times 10^{-5}T \quad (16)$$

where ρ is in $\mu\Omega\,\mathrm{m}$ and T in K.

For Fig. 5 electrical resistivity from Fig. 4 is compensated for thermal expansion as a function of temperature by considering literature values of the thermal expansion for platinum, in the solid from Blanke [20] and in the liquid from Gathers et al. [8] as well as from Hixson and Winkler [17]. The change of diameter results in a shift to higher resistivity values, as the actual cross-section of the wire, which also is responsible for electrical resistivity, is increased. At the onset of melting, which is indicated with a vertical dotted line, we obtain a value of $0.647\,\mu\Omega\,\mathrm{m}$ and at the end of melting a value of $1.012\,\mu\Omega\,\mathrm{m}$ for volume adjusted resistivity. Thus an increase of $\Delta\rho = 0.365\,\mu\Omega\,\mathrm{m}$ at melting is observed. The polynomial fit to our volume adjusted values (index v) for the solid in the temperature range $473\,\mathrm{K} < T < 1600\,\mathrm{K}$ is

$$\rho_\mathrm{v} = -0.01633 + 4.39347 \times 10^{-4}T - 5.69652 \times 10^{-8}T^2 \quad (17)$$

and for $1740\,\mathrm{K} < T < 2042\,\mathrm{K}$ is

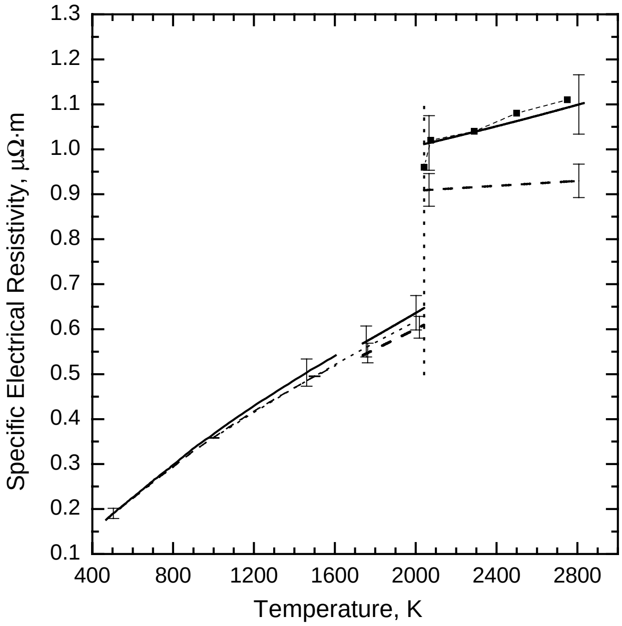

Fig. 5. Electrical resistivity of platinum resistivity without taking actual volume in account, and with volume expansion taken into consideration, versus temperature. Solid line: electrical resistively adapted for volume expansion; dashed line: electrical resistivity without volume correction. Both lines are least-squares fits to measured data. Dashed dotted line data of Hixson and Winkler [17]; full squares: data of Hixson and Winkler [17]. Vertical dotted line: melting temperature (2042 K); dashed line: literature values from [11] without volume correction.

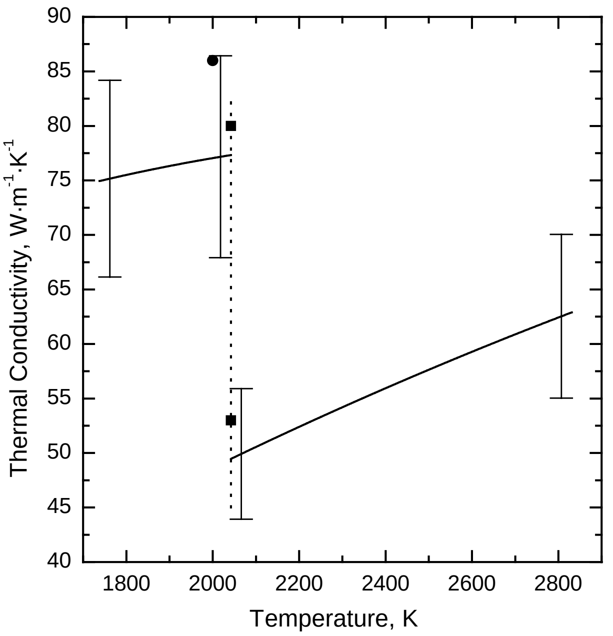

Fig. 6. Thermal conductivity of platinum versus temperature. Solid lines: linear least-squares fit to measured data (average of 11 measurements); vertical dotted line: melting temperature (2042 K); full squares: literature values for the melting transition from [7]; full circle: value from [21].

$$\rho_{\mathrm{v}} = 0.160911 + 2.13157 \times 10^{-4}T + 1.21855 \times 10^{-8}T^2 \quad (18)$$

and for the liquid in the temperature range $2042\,\mathrm{K} < T < 2900\,\mathrm{K}$

$$\rho_{\mathrm{v}} = 0.842393 + 5.92611 \times 10^{-5}T + 1.15438 \times 10^{-8}T \quad (19)$$

where ρ_{v} is in $\mu\Omega\,\mathrm{m}$ and T in K.

Fig. 6 presents thermal conductivity versus temperature. To estimate thermal conductivity via Eq. (4) the density data reported from [8,17,20] have been used to correct electrical resistivity for the actual thermal expansion. The square fit for the solid in the temperature range $1750\,\mathrm{K} < T < 2042\,\mathrm{K}$ is

$$\lambda = 44.0544 + 2.62416 \times 10^{-2}T - 4.87228 \times 10^{-6}T^2 \quad (20)$$

for the liquid in the temperature range $2042\,\mathrm{K} < T < 2900\,\mathrm{K}$ is

$$\lambda = 0.344146 + 2.91170 \times 10^{-2}T - 2.47995 \times 10^{-6}T^2 \quad (21)$$

where λ is in $\mathrm{W\,m^{-1}\,K^{-1}}$ and T in K.

We obtain at the onset of melting a value of $77.3\,\mathrm{W\,m^{-1}\,K^{-1}}$ and at the end of melting for the beginning of the liquid phase a value of $49.5\,\mathrm{W\,m^{-1}\,K^{-1}}$. Mills et al. [7] report for the end of the solid phase $80\,\mathrm{W\,m^{-1}\,K^{-1}}$, respectively, $53\,\mathrm{W\,m^{-1}\,K^{-1}}$ for the begin of the liquid phase, Zinov'yev [21] reports for the end of the solid phase $86\,\mathrm{W\,m^{-1}\,K^{-1}}$.

Thermal diffusivity can be estimated from thermal conductivity using Eq. (4). The graph thermal diffusivity versus temperature is not plotted here, the corresponding fit for the solid in the temperature range from 1750 to 2042 K is

$$a = 1.11214 \times 10^{-5} + 7.30502 \times 10^{-9}T - 1.14827 \times 10^{-12}T^2 \quad (22)$$

for the liquid in the temperature range from 2042 to 2900 K is

$$a = 8.29065 \times 10^{-8} + 7.04056 \times 10^{-9}T - 1.81439 \times 10^{-13}T^2 \quad (23)$$

where a is in $\mathrm{m^2\,s^{-1}}$ and T in K.

We obtain at the onset of melting a value for a of $2.1 \times 10^{-5}\,\mathrm{m^2\,s^{-1}}$ and at the end of melting for the beginning of the liquid phase a value of $1.4 \times 10^{-5}\,\mathrm{m^2\,s^{-1}}$.

6. Discussion

Platinum is a material, where at the first time a jump of normal spectral emissivity at melting has been observed when using the samples as received. If one polishes the sample with abrasive paper (e.g. 1000 grids) in the solid phase a higher emissivity value will be observed and at melting a drop of normal spectral emissivity will occur. This demonstrates that normal spectral emissivity of the solid sample strongly depends of the surface conditions, whereas for the liquid sample surface always repeatable results are obtained. From Fig. 1 the maximum difference between "true temperature" and temperature calculated with a constant emissivity at melting and in the liquid phase is found to be not more than 1.5%. Thus, for thermophysical properties of liquid platinum reported in literature, e.g. [17] so far under the assumption of the same emissivity during melting and during the liquid phase no major corrections are necessary.

The comparison of normal spectral emissivity at 684.5 nm in the melting region gives a good agreement to values reported in literature as depicted in Fig. 2. There are three literature values [12,13,23] at the end of melting in the range of 0.36–0.38 and one at the onset of melting [11], which all fit quite well to the values of this work. Furthermore, emissivity values from melting up to 3000 K are presented for liquid platinum, which are only slightly increasing.

Heat of fusion and specific heat capacity for liquid platinum are compared to literature data within Fig. 3. There is a good agreement to literature values at the melting transition, as presented in Table 1. For the liquid data of enthalpy versus temperature a larger scatter can be observed, but it is still within the stated uncertainty of such pulse heating experiments. For verifying the quality of the measured values obtained with the pulse heating experiment in the solid phase, measurements with a differential scanning calorimeter for platinum were performed and are depicted in Fig. 3. This polynomial was extrapolated up to the melting point of platinum (2042 K) and finally integrated over temperature. The enthalpy at 298 K is set to zero. In the solid, our values obtained by pulse heating match within the stated uncertainties excellently the measured DSC values. Thus within Fig. 3 the interval of data ranges from 473 to 2830 K.

For electrical resistivity with thermal expansion considered versus temperature in Fig. 4 we state a good agreement to literature values in the solid and at the melting transition. Due to our DSC measurements we could extend the range of data in the solid phase from melting down to 473 K. The comparison to data of Zinov'yev [21] gives excellent agreement in the solid phase. This extension due to the DSC measurements is a major improvement, as the pulse heating results would start at a temperature of about 1700 K.

In Fig. 5 the change of volume due to thermal expansion is considered to obtain actual resistivity values for liquid platinum in the range from 473 to 2830 K and results in a slight increase of resistivity values in the solid. For the liquid there is a larger increase of resistivity due to expansion.

For fast pulse experiments, expansion of the sample only occurs in radial direction, as can be seen by short-time pictures of the expanding sample [24]. An expansion into axial direction would result in bending of the wire which can only be observed if the applied heating rates are to slow. The liquid resistivity data are compared to Hixson and Winkler [17] and give an excellent agreement.

In Fig. 6 thermal conductivity was estimated using the Wiedemann–Franz law. Our values match well with those reported in literature [7,21] for the melting transition. In the liquid, where direct measurements of thermal conductivity are almost impossible, the calculation from electrical resistivity is one of the rare methods of an indirect approximation. Further an estimate of thermal diffusivity in this temperature region is given in form of a polynomial fit.

7. Uncertainties

According to the guide to the expression of uncertainty in measurement [22] uncertainties reported here are expanded relative uncertainties with a coverage factor of $k = 2$. Two lists of final evaluated sets of uncertainties are given, first for the actuating variables such as: current (I), 2%; voltage drop (U), 2%; temperature (T), 4%, normal spectral emissivity (ε), 6%; mass (m), 2%, and second for the measured variables obtained according to Eqs. (1)–(8): enthalpy (H), 4%; enthalpy of melting (ΔH), 8%, specific heat capacity (c_p), 8%, not volume-corrected specific electrical resistivity ($\rho_{\mathrm{el,uncorr}}$), 4%; $\rho_{\mathrm{el,corr}}$, 6%; thermal conductivity (λ), 12% and thermal diffusivity (a), 16%. Within the figures the actual uncertainty bars are depicted.

8. Conclusions

The emissivity values determined within this work by means of a four detector polarimetry for liquid platinum at 684.5 nm do not lead to major corrections in the thermophysical property values reported in the literature up to now for liquid platinum. Within this work the remaining ambiguity was eliminated by simultaneous optical property, apparent temperature and thermophysical property, measurement on pulse-heated liquid platinum samples. By means of DSC measurements and pulse heating, the reported thermophysical data of platinum could be extended from 473 to 2830 K.

Acknowledgements

Research supported by FWF Grant P15055.

References

[1] NIST, Standard Reference Data Program, Online Databases, Chemistry WebBook. http://webbook.nist.gov/cgi/cbook.cgi?ID=C7440064&Units=SI&Mask=6.
[2] V. Gutmann, E. Hengge, Anorganische Chemie: eine Einführung, 5. Auflage, VCH, Weinheim, New York, Basel, Cambridge, 1990.
[3] E. Kaschnitz, G. Pottlacher, H. Jäger, Int. J. Thermophys. 13 (1992) 699–710.
[4] A. Seifter, G. Pottlacher, H. Jäger, G. Groboth, E. Kaschnitz, Ber. Bunsenges. Phys. Chem. 102 (1998) 1266–1271.
[5] A. Seifter, F. Sachsenhofer, S. Krishnan, G. Pottlacher, Int. J. Thermophys. 22 (2001) 1537–1547.
[6] Advent Research Materials Periodic Table. http://www.advent-rm.com/periodictable.asp.
[7] K.C. Mills, B.J. Monaghan, B.J. Keene, Thermal Conductivities of Molten Metals, Part 1, Pure Metals, NPL Report CMMT(A), 1997, p. 53.
[8] G.R. Gathers, J.W. Shaner, W.M. Hodgson, High Temp. High Press. 11 (1979) 529–538.
[9] J.L. Margrave, High Temp. High Press. 2 (1970) 583–586.
[10] G. Pottlacher, A. Seifter, Int. J. Thermophys. 23 (2002) 1281–1291.
[11] F. Righini, A. Rosso, High Temp. High Press. 12 (1980) 335–349.
[12] J.L. McClure, A. Cezairliyan, E. Kaschnitz, Int. J. Thermophys. 20 (1999) 1149–1161.
[13] S. Krishnan, G.P. Hansen, R.H. Hauge, J.L. Margrave, High Temp. Sci. 29 (1990) 17–52.
[14] A.H. Seville, J. Chem. Thermodyn. 7 (1975) 383–387.
[15] R. Hultgren, P.D. Desai, D.T. Hawkins, M. Gleiser, K.K. Kelley, D.D. Wagman, Selected Values of the Thermodynamic Properties of the Elements, American Society for Metals, 1973.
[16] A.K. Chaudhuri, D.W. Bonell, L.A. Ford, J.L. Margrave, High Temp. Sci. 2 (1970) 203–212.
[17] R.S. Hixson, M.A. Winkler, Int. J. Thermophys. 14 (1993) 409–416.
[18] M.M. Martynyuk, V.I. Tsapkov, Fiz. Metal. Metalloved. 37 (1974) 49–54.

[19] S.V. Lebedev, A.I. Savvatimskii, Y.B. Smirnov, Trans. Teplofizika Vysokikh Temperatur 9 (1971) 653–683.

[20] W. Blanke (Ed.), Thermophysikalische Stoffdaten, Springer-Verlag, Berlin, 1989.

[21] V.E. Zinov'yev, Metals at High Temperatures—Standard Handbook of Properties, National Standard Reference Data Service of the USSR, Hemisphere Publishing Corporation, 1990.

[22] Expression of the Uncertainty of Measurement in Calibration, EA-4/02. http://www.european-accreditation.org/pdf/EA-4-02ny.pdf.

[23] T. Baykara, R.H. Hauge, N. Norem, P. Lee, J.L. Margrave, High Temp. Sci. 32 (1991) 113–154.

[24] C. Otter, G. Pottlacher, H. Jäger, Int. J. Thermophys. 17 (1996) 987–1000.